Subdivisions of Ring Dupin Cyclides Using Bézier Curves with Mass Points

Lionel Garnier, Lucie Druoton, Jean-Paul Becar, Laurent Fuchs, Géraldine Morin

Subdivisions of Ring Dupin Cyclides Using B®zier Curves with Mass Points

LIONEL GARNIER[1], LUCIE DRUOTON[2], JEAN-PAUL BÉCAR[3]
LAURENT FUCHS[4], GÉRALDINE MORIN[5]

[1]L.I.B., University of Burgundy, B.P. 47870, 21078 Dijon Cedex, France;
[2]I.U.T. of Dijon, University of Burgundy-Franche-Comté, B.P. 47870, 21078 Dijon Cedex, France ;
[3]U.P.H.F. - Campus Mont Houy - 59313 Valenciennes Cedex 9, France;
[4]X.L.I.M., U.M.R. 7252, University of Poitiers, France;
[5]Laboratoire IRIT, U.M.R. 5505, University Paul Sabatier, 31 000 Toulouse, France;

Abstract: The paper deals in the Computer-Aided Design or Computer-Aided Manufacturing domain with the Dupin cyclides as well as the Bézier curves. It shows that the same algorithms can be used either for subdivisions of ring Dupin cyclides or Bézier curves. The Bézier curves are described with mass points here. The Dupin cyclides are considered in the Minkowski-Lorentz space. This makes a Dupin cyclide as the union of two conics on the unit pseudo-hypersphere, called the space of spheres. And the conics are quadratic Bézier curves modelled by mass points. The subdivision of any Dupin cyclide, is equivalent to subdivide two curves of degree 2, independently, whereas in the 3D Euclidean space, the same work implies the subdivision of a rational quadratic Bézier surface and resolutions of systems of three linear equations. The first part of this work is to consider ring Dupin cyclides because the conics are bounded circles which look like ellipses.

Key-Words: Mass points, Rational quadratic Bézier curves, Conics, Subdivisions, Space of spheres, Minkowski-Lorentz space, Ring Dupin cyclides

Received: April 23, 2021. Revised: October 9, 2021. Accepted: October 23, 2021. Published: November 9, 2021.

1 Introduction

Dupin cyclides are algebraic surfaces introduced in 1822 by the french mathematician Pierre-Charles Dupin [1] and were introduced in Computer Aided Design (C.A.D.) by R. Martin in 1982 [2]. They have a low algebraic degree: at most 4. These Dupin cyclides have a parametric equation and two equivalent implicit equations [3, 4] and they have been studied by a lot of mathematicians [4, 5, 6]. Since a score of years, much of authors used them in Computer Aided Geometric Design (C.A.G.D.). In previous studies [7, 8, 9, 10], Dupin cyclides are represented by Rational Biquadratic Bézier Surfaces (R.B.B.S.) in the usual 3D Euclidean affine space $\mathcal{E}_3$. Four patches are necessary to model the whole cyclide. Then, the conditions of the control points of a R.B.B.S. that can represent a Dupin cyclide patch have been given [11, 12, 13, 14, 15, 16]. A similar construction is possible in the space of spheres [17].

In C.A.D., rational Bézier curves are the basis for the standard Non-Uniform Rational Bézier Splines (N.U.R.B.S.) representation. In particular, second order rational Bézier curves model conic arcs [18, 19, 14, 20]. However, since point on Bézier curve are expressed as barycenters of a set of the control points, they are, in the classical setting, limited to modeling bounded arcs. Unbounded conics arcs, like parabola or hyperbola branches, may be modeled by considering the joint space of weighted points and vectors [21]. In this space, vectors correspond to points associated the weight zero. Here, we propose to further investigate this general setting to propose an original subdivision algorithm for bounded and unbounded conic arcs[1] and the subdivision is independent of the rational parameterization. The subdivision

[1]The work will be presented in a future paper.

theorems in Paragraph 4, lay on Theorem 5 which offers to change mass points. The Theorem 5 in B.2.3 and his Corollary 1 give a way to build a conic arc that eases the calculation of the conic invariants [20, 22, 23].

The space of spheres was introduced in various ways. For example, M. Berger [6] works in the projective space of the quadratic forms on the affine Euclidean space, M. Paluszny [24] works in a four dimensional projective space using the hypersphere of Moebius. While U. Hertrich-Jeromin [25], T. Cecil [26], R. Langevin and P. Walczak [27] use a four dimensional quadric Λ^4 in the five dimensional Minkowski-Lorentz space which is endowed with a non-degenerate indefinite quadratic form of signature $(4,1)$. That space is a generalization of the space-time used in Einstein's theory, equipped of the non-degenerate indefinite quadratic form

$$\mathcal{Q}_M\left(\overrightarrow{u}\right) = x^2 + y^2 + z^2 - c^2\,t^2$$

where (x, y, z) are the spacial components of the vector $\overrightarrow{u}$ and t is the time component of $\overrightarrow{u}$ and c is the constant of the speed of light. The Minkowski-Lorentz space permits to solve the three contact condition problem [28] whereas the other space leads to nothing: with the projective spaces, the orientations of the spheres are lost. In these projective space, from two spheres of centers O_0 and O_1 and of non-null radius r, we can not distinguish a cone and a cylinder. In the Minkowski-Lorentz spheres, the two spheres of centers O_0 and O_1 and of non-null radius r lead to a circular cylinder whereas the sphere of center O_0 and of radius r and a sphere of center O_1 and radius $-r$ lead to a circular cone.

In the Minkowski-Lorentz space, a Dupin cyclide is the union of two conics, see Definition 1 and Table 1. We can choose a vector using perpendicular conditions and pseudo-metric conditions to determine a Bézier curve which models a circle for the non-degenerate indefinite quadratic form and this circle looks like an ellipse or hyperbola with an Euclidean point of view. Some recalls about the Minkowski-Lorentz spaces $\mathrm{L}_{4,1}$ and $\overrightarrow{\mathrm{L}_{4,1}}$ can be found in [29, 30, 31, 32, 33, 34, 17, 28]. Some formulae are given in Appendix A. The use of Minkowski-Lorentz space permits to simplify the subdivision algorithms developed by L. Garnier and C. Gentil [15]. One can note that an inversion is not an affine, transformation and so, the control points of the image of a Bézier curve are not the images of the control points of the original Bézier curve. Then, the general Dupin cyclide case and torus case must be distinguish. Some recalls about mass points and Bézier curves can be found in [21, 35, 36, 29, 30], to facilitate the read of this paper, some formulae are given in Appendix B.

The paper is organized as follows: Section 2 presents Dupin cyclides in the 3-dimensional Euclidean affine space $\mathcal{E}_3$ and in the Minkowkski-Lorentz space. In section 3, the authors present the adaptation of De Casteljau algorithm to Bézier curves with mass points. Section 4 presents methods to subdivide Bézier curves which model ellipse arcs and then Ring Dupin Cyclide. Before the conclusion and the perspectives, in section 5, the authors present the method to subdivide Ring Dupin cyclides patches. The Appendix A (resp. B) presents some fundamental recalls about Minkowski-Lorentz space (resp. Bézier curves with mass points) to clarify this paper.

2 Dupin cyclide in the Minkowkski-Lorentz space

An Euclidean sphere S of the 3-dimensional usual affine Euclidean space $\mathcal{E}_3$ of center Ω and of radius r defines two oriented spheres S^+ and S^- of center Ω and of radius $\rho = r$ and $\rho = -r$ respectively. For any point M belonging to the sphere S^+ or S^-, we have

$$\overrightarrow{\Omega M} = \rho\overrightarrow{N} \tag{1}$$

where $\overrightarrow{N}$ is the unit normal vector to the considered sphere at the point M.

The space of spheres Λ^4 is the 4-dimensional pseudo-unit hypersphere of the Minkowkski-Lorentz space, see Appendix A.

Dupin cyclides can be defined in different ways [4, 3]. Using the space of spheres in the Minkowski-Lorentz space, we use the following definition:

Definition 1 :

A Dupin cyclide is, in two different ways, the envelope of an one-parameter family of oriented spheres. Each family of spheres can be seen as a conic in the space of spheres Λ^4. These two conics are called brother circles.

We can distinguish five kinds of Dupin cyclides and the type of the conic in the Minkowkski-Lorentz space depends of the number of singular points of these surfaces [2, 7, 37, 38], see Table 1. A Ring Dupin cyclide is a Dupin cyclide without singular points, see Fig. 1.

The representation of a Ring Dupin cyclide in the space of spheres Λ^4 is the union of two circles which look like ellipses (with an Euclidean point of view), Fig. 2. In a second paper, we will deal

Table 1: Kinds of Dupin cyclides and their representations in the Minkowski-Lorentz space.

Name of Dupin cyclide	Number of singular point(s)	Lorentz property	Euclidean point of view
Ring	0	Two circles	Two ellipses
Horned Spindle	2	Two circles	An ellipse and a hyperbola
One-singularity spindle Singly horned	1	A circle and a parabola	An ellipse and a parabola

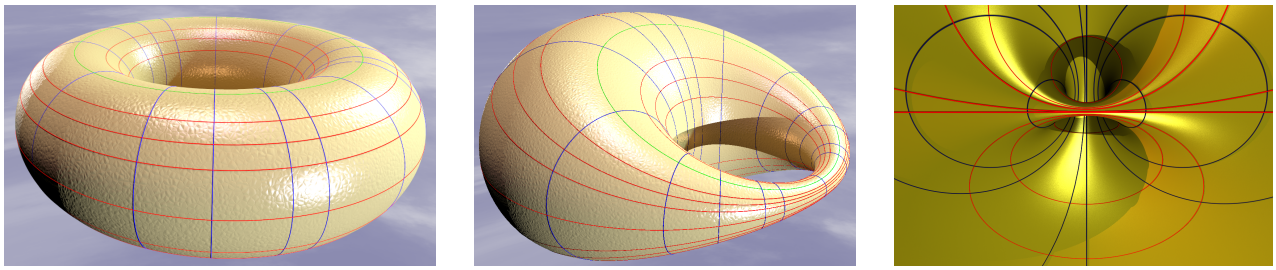

(a) (b) (c)

Figure 1: Three ring Dupin cyclides in $\mathcal{E}_3$. (a): torus. (b): general quartic Dupin cyclide. (c): cubic Dupin cyclide.

with the other Dupin cyclides represented by a circle which looks like an ellipse and an other conic: a circle which looks like a hyperbola or an affine parabola isometric to a line [39]. For i in $\{1,2\}$, let Ω_i be the center of the circle C_i which is contained into the affine 2-plane $\mathcal{P}_i$. Then, the planes $\mathcal{P}_i$ and $\mathcal{P}_{3-i}$ are perpendicular, the line $(\Omega_1\Omega_2)$ is perpendicular to $\mathcal{P}_i$.

From the Minkowski-Lorentz spaces, the set $\widetilde{L_{4,1}}$ of mass points (A,a) are defined, see Appendix B, where

- $a=0$ implies that A is a vector of $\overrightarrow{L_{4,1}}$;
- $a\neq 0$ implies that A is a point of $L_{4,1}$.

3 The De Casteljau algorithm adapted to $\widetilde{L_{4,1}}$

A recall about the rational quadratic Bézier curve with mass points of control $(P_0;\omega_0)$, $(P_1;\omega_1)$ and $(P_2;\omega_2)$ is done in Appendix B.2. To simplify the rest of this paper, we introduce the following notation:

Notation 1 :
$BR\{(P_0;\omega_0);(P_1;\omega_1);(P_2;\omega_2)\}$ denotes a rational quadratic Bézier curve with the following control mass points $(P_0;\omega_0)$, $(P_1;\omega_1)$ and $(P_2;\omega_2)$.

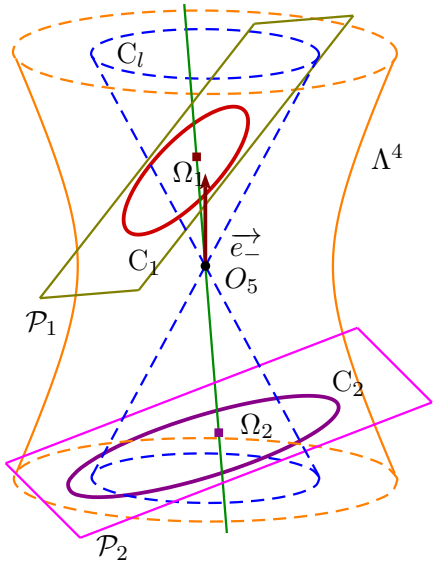

Figure 2: Representation of a ring Dupin cyclide on Λ^4: the two brother circles C_1 and C_2 look like ellipses.

Given that the law $\oplus$, defined in Appendix B, is associative, the De Casteljau algorithm can be generalized to the Bézier curve in the space of mass points, Algorithm 1.

Algorithm 1 The De Casteljau algorithm in the space of mass points.

Input : Three mass points $(P_0;\omega_0)$, $(P_1;\omega_1)$ and $(P_2;\omega_2)$ not collinear.

1. Choice of t in $]0;1[$
2. Calculation of:
   $(N_1;\varpi_1) = (1-t)\odot(P_0;\omega_0)\oplus t\odot(P_1;\omega_1)$
3. Calculation of:
   $(N_2;\varpi_2) = (1-t)\odot(P_1;\omega_1)\oplus t\odot(P_2;\omega_2)$
4. Calculation of:
   $(N_3;\varpi_3) = (1-t)\odot(N_1;\varpi_1)\oplus t\odot(N_2;\varpi_2)$

Output : A mass point $(N_3;\varpi_3)$ belonging to the conic arc modeled by $BR\{(P_0;\omega_0);(P_1;\omega_1);(P_2;\omega_2)\}$

From Algorithm 1, it yields:

$$\begin{array}{rcl}(N_3;\varpi_3) & = & B_0(t)\odot(P_0;\omega_0)\\ & \oplus & B_1(t)\odot(P_1;\omega_1)\\ & \oplus & B_2(t)\odot(P_2;\omega_2)\end{array} \tag{2}$$

In the following, we point out regular subdivisions (e.g. $t_0=\frac{1}{2}$ in Algorithm 1) and distinguish weighted points and vectors. It is not possible to obtain directly this result with the Algorithm 1 : given that for each step of iteration the weights added implies a disturbance, see [40]. The use of Theorem 5 or the Corollary 1, see B.2.3 or [20, 23], provides a regular subdivision (the weighted point N_3 belongs to the $\mathcal{L}_{4,1}$-perpendicular bisector from P_1 in the triangle $P_0P_1P_2$). We impose that:

- if the endpoint is a weighted point, its weight equals 1;
- if the endpoint is a vector, its first component is 1, see Table 2 in Appendix A.2. The representation of a point $M_0(x_0,y_0,z_0)\in\mathcal{E}_3$ in the Minkowski-Lorentz space is the light-like vector $\overrightarrow{m_0}\left(1,x_0,y_0,z_0,\frac{x_0^2+y_0^2+z_0^2}{2}\right)\in\overrightarrow{\mathrm{L}_{4,1}}$.

Moreover if $(N_3;\varpi_3)$ is a weighted point the straight line defined by the mass points $(N_3;\varpi_3)$ and $(N_1;\varpi_1)$ or $(N_2;\varpi_2)$ represent the tangent line to the BR curve at N_3.

4 Regular iterative subdivision of Dupin cyclides or Bézier curves

Using the Theorem 5 or the Corollary 1, we define two homographies h_0 and h_1 from $[0;1]$ into $\left[0;\frac{1}{2}\right]$ and $\left[\frac{1}{2};1\right]$ respectively. For i in $[\![0;1]\!]$, h_i is defined by four real numbers and we have two degrees of freedom. Let us give more details about these homographies.

4.1 Homography h_0

We have

$$h_0(u)=\frac{a_0\,(1-u)+b_0\,u}{c_0\,(1-u)+d_0\,u} \tag{3}$$

and we have to solve

$$\left\{\begin{array}{rcl}h_0(0) & = & 0\\ h_0(1) & = & \frac{1}{2}\end{array}\right. \tag{4}$$

which leads to

$$\left\{\begin{array}{rcl}a_0 & = & 0\\ d_0 & = & 2\,b_0\end{array}\right. \tag{5}$$

and the homography becomes

$$h_0(u)=\frac{b_0\,u}{c_0\,(1-u)+2\,b_0\,u} \tag{6}$$

with $(b_0,c_0)\in(\mathbb{R}^+)^2$.

Let $(P_0;\omega_0)$, $(P_1;\omega_1)$ and $(P_2;\omega_2)$ be the control mass points of the Bézier curve γ. Using the Theorem 5, the control mass points of the Bézier curve $\gamma\circ h_0$ are $(Q_0;\varpi_0)$, $(Q_1;\varpi_1)$ and $(Q_2;\varpi_2)$ with

$$\left\{\begin{array}{rcl}(Q_0;\varpi_0) & = & c_0^2\odot(P_0;\omega_0)\\ (Q_1;\varpi_1) & = & c_0\,b_0\odot(P_0;\omega_0)\\ & \oplus & b_0\,c_0\odot(P_1;\omega_1)\\ (Q_2;\varpi_2) & = & b_0^2\odot(P_0;\omega_0)\\ & \oplus & 2\,b_0^2\odot(P_1;\omega_1)\\ & \oplus & b_0^2\odot(P_2;\omega_2)\end{array}\right. \tag{7}$$

Since we want that the first control mass point of the two curves γ and $\gamma\circ h_0$ is the same, we have $c_0=1$. If $\omega_0+2\,\omega_1+\omega_2\neq 0$, the last control mass point is a weighted point, in order to have $\varpi_2=1$, we choose

$$b_0=\frac{1}{\sqrt{\omega_0+2\,\omega_1+\omega_2}} \tag{8}$$

else the computation of b_0 depends on the vector $\overrightarrow{Q_2}$: either $\overrightarrow{Q_2}$ is $\overrightarrow{e_\infty}$ or its first component equals 1.

4.2 Homography h_1

In the same way, we have

$$h_1(u) = \frac{a_1\,(1-u) + b_1\,u}{c_1\,(1-u) + d_1\,u} \tag{9}$$

and we have to solve

$$\left\{ \begin{array}{rcl} h_1(0) & = & \dfrac{1}{2} \\ h_1(1) & = & 1 \end{array} \right. \tag{10}$$

which leads to

$$\left\{ \begin{array}{rcl} c_1 & = & 2\,a_1 \\ d_1 & = & b_1 \end{array} \right. \tag{11}$$

and the homography becomes

$$h_1(u) = \frac{a_1\,(1-u) + b_1\,u}{2\,a_1\,(1-u) + b_1\,u} \tag{12}$$

with $(a_1, b_1) \in (\mathbb{R}^+)^2$.

Let $(P_0;\omega_0)$, $(P_1;\omega_1)$ and $(P_2;\omega_2)$ be the control mass points of the Bézier curve γ. Using the Theorem 5, the control mass points of the Bézier curve $\gamma \circ h_1$ are $(Q_0;\varpi_0)$, $(Q_1;\varpi_1)$ and $(Q_2;\varpi_2)$ with

$$\left\{ \begin{array}{rcl} (Q_0;\varpi_0) & = & a_1^2 \odot (P_0;\omega_0) \\ & \oplus & 2\,a_1^2 \odot (P_1;\omega_1) \\ & \oplus & a_1^2 \odot (P_2;\omega_2) \\ (Q_1;\varpi_1) & = & a_1\,b_1 \odot (P_1;\omega_1) \\ & \oplus & a_1\,b_1 \odot (P_2;\omega_2) \\ (Q_2;\varpi_2) & = & b_1^2 \odot (P_2;\omega_2) \end{array} \right. \tag{13}$$

Since we want that the last control mass point of the two curves γ and $\gamma \circ h_1$ is the same, we have $b_1 = 1$. If $\omega_0 + 2\,\omega_1 + \omega_2 \neq 0$, the first control mass point is a weighted point, in order to have $\varpi_0 = 1$, we choose

$$a_1 = \frac{1}{\sqrt{\omega_0 + 2\,\omega_1 + \omega_2}} \tag{14}$$

else the computation of a_1 depends on the vector $\overrightarrow{Q_0}$: either $\overrightarrow{Q_0}$ is $\overrightarrow{e_\infty}$ or its first component is 1.

From Table 4, one can see that Bézier curves are ellipse arcs if the weights $(\omega_0;\omega_1;\omega_2)$ belong to $\{1\} \times]-1, 1[\times \{1\}$.

4.3 Subdivision methods

We distinct two cases:

1. the segment $[P_0P_2]$ is not a diameter of the ellipse[2] and the intermediate control mass point is a weighted point;
2. the Bézier curve is a semi-ellipse[3] and the intermediate control mass point is a vector.

Since the rational quadratic Bézier curve with mass points of control $(P_0;\omega_0)$, $(P_1;\omega_1)$ and $(P_2;\omega_2)$ is a circle arc in the Minkowski-Lorentz space and an ellipse arc in the usual Euclidean affine plane, our methods do not depend on the metric of the space.

4.3.1 Case with 3 weighted points : $(\omega_0;\omega_1;\omega_2) \in \{1\} \times]-1, 1[- \{0\} \times \{1\}$

Let us recall that

$$Bar\,\{(A_k;\omega_k)\}$$

designates the barycentre of the weighted points $\{(A_k;\omega_k)\}$.

Theorem 1 Let γ be a Bézier curve with control mass points $(\sigma_0;1)$, $(P_1;\omega_1)$ and $(\sigma_2;1)$ laying on the conic C.

Let $h_0 : [0,1] \to \left[0, \frac{1}{2}\right]$ defined by :

$$h_0 : u \longmapsto \frac{\dfrac{1}{\sqrt{2+2\omega_1}}\,u}{(1-u) + 2\,\dfrac{1}{\sqrt{2+2\omega_1}}\,u} \tag{15}$$

then $\gamma \circ h_0$ equals a Bézier curve with control mass points $(\sigma_{00};1)$, $(P_{10};\varpi_{10})$ and $(\sigma_{20};1)$ laying on the conic C with :

$$\left\{ \begin{array}{c} (\sigma_{00};1) = (\sigma_0;1) \\ P_{10} = Bar\,\{(\sigma_0;1)\,;(P_1;\omega_1)\} \\ \varpi_{10} = \sqrt{\dfrac{1+\omega_1}{2}} \\ \sigma_{20} = Bar\,\{(\sigma_0;1)\,;(P_1;2\,\omega_1)\,;(\sigma_2;1)\} \\ \varpi_{10} = 1 \end{array} \right. \tag{16}$$

Proof: by the use of Formula (7) with

$$b_0 = \frac{1}{\sqrt{2+2\omega_1}}$$

and $c_0 = 1$.

■

Note that $\varpi_1 = \sqrt{\frac{1+\omega_1}{2}}$ is the well known the recurrence equation in the Euclidean case. For symmetry reasons, we can formulate,

[2]The curve is a circle for the Lorentz metric in $L_{4,1}$

[3]The curve is a semi-circle for the Lorentz metric in $L_{4,1}$

Theorem 2 Let γ be a Bézier curve with control mass points $(\sigma_0;1)$, $(P_1;\omega_1)$ and $(\sigma_2;1)$ laying on the conic C.

Let $h_1 : [0,1] \to \left[\frac{1}{2},1\right]$ defined by

$$h_1 : u \longmapsto \frac{\dfrac{1}{\sqrt{2+2\omega_1}}(1-u)+u}{2\dfrac{1}{\sqrt{2+2\omega_1}}(1-u)+u} \tag{17}$$

then $\gamma \circ h_1$ equals a Bézier curve with control mass points $(\sigma_{01};1)$, $(P_{11};\varpi_{11})$ et $(\sigma_{21};1)$ laying on the conic C with :

$$\begin{cases} \sigma_{01} = Bar\left\{(\sigma_0;1);(P_1;2\,\omega_1);(\sigma_2;1)\right\} \\ \varpi_{01} = 1 \\ P_{11} = Bar\left\{(P_1;\omega_1);(\sigma_2;1)\right\} \\ \varpi_{11} = \sqrt{\dfrac{1+\omega_1}{2}} \\ (\sigma_{21};1) = (\sigma_2;1) \end{cases} \tag{18}$$

The Fig. 3 shows an iteration of the subdivision algorithm based on theorems 1 and 2 thus we have $\sigma_{20} = \sigma_{01}$, $\sigma_0 = \sigma_{00}$ and $\sigma_2 = \sigma_{21}$. The Bézier curve of control mass points $(\sigma_0;1)$, $(P_1;\omega_1)$ and $(\sigma_2;1)$ is subdivided into two Bézier curves $\gamma \circ h_0$ and $\gamma \circ h_1$. The control mass points of $\gamma \circ h_0$ are $(\sigma_{00};1)$, $(P_{10};\omega_1)$ and $(\sigma_{20};1)$. The control mass points of $\gamma \circ h_1$ are $(\sigma_{01};1)$, $(P_{01};\omega_1)$ and $(\sigma_{21};1)$.

4.3.2 Case of two endpoints and a intermediate vector: $(\omega_0;\omega_1;\omega_2) = (1;0;1)$

The curve in the Minkowski-Lorentz space is a semi-circle which looks like an Euclidean semi-ellipse. The endpoints of the Bézier curve are the weighted points $(\sigma_0;1)$ and $(\sigma_2;1)$, the intermediate control mass point is the vector $\left(\overrightarrow{P_1};0\right)$ and we have

$$\begin{cases} 4\,\overrightarrow{P_1}^2 &= \overrightarrow{\sigma_2\sigma_0}^2 \\ \overrightarrow{P_1}\,.\,\overrightarrow{\sigma_2\sigma_0} &= 0 \end{cases} \tag{19}$$

Theorem 3 Let a Bézier curve γ with control mass points $(\sigma_0;1)$, $\left(\overrightarrow{P_1};0\right)$ and $(\sigma_2;1)$ laying on the conic C.

Let Ω_1 be the midpoint of the segment $[\sigma_0;\sigma_2]$.

Let h_0 defined by

$$h_0 : u \longmapsto \frac{\dfrac{\sqrt{2}}{2}u}{(1-u)+\sqrt{2}\,u} \tag{20}$$

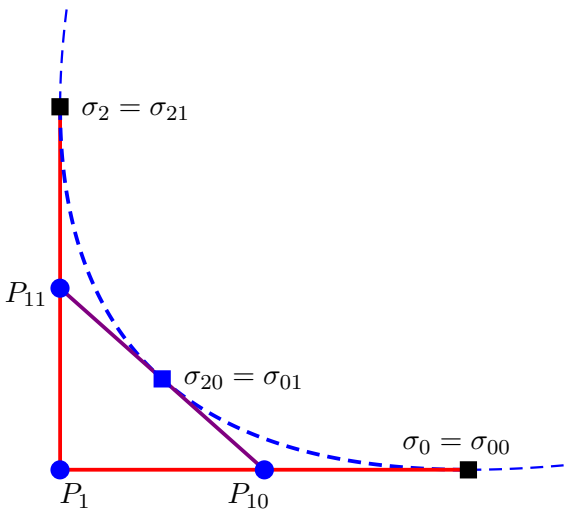

Figure 3: One step of an iterative subdivision of a conic arc γ on Λ^4. The endpoints are σ_0 and σ_2. The tangent lines at the endpoints are the straight lines $(\sigma_0 P_1)$ and $(\sigma_2 P_1)$ where the weighted point $(P_1;\omega_1)$ verifies $0 < |\omega_1| < 1$.

then $\gamma \circ h_0$ is a Bézier curve with control mass points $(\sigma_{00};1)$, $(P_{10};\varpi_{10})$ and $(\sigma_{20};1)$ laying on the conic C with:

$$\begin{cases} (\sigma_{00};1) &= (\sigma_0;1) \\ (P_{10};\varpi_{10}) &= \left(\mathcal{T}_{\overrightarrow{P_1}}(\sigma_0);\dfrac{\sqrt{2}}{2}\right) \\ (\sigma_{20};1) &= \left(\mathcal{T}_{\overrightarrow{P_1}}(\Omega_1);1\right) \end{cases} \tag{21}$$

Proof: by the use of Formula (7) with $b_0 = \frac{\sqrt{2}}{2}$ and $c_0 = 1$.

■

For symmetric reasons, we can formulate

Theorem 4 Let a Bézier curve γ with control mass points $(\sigma_0;1)$, $\left(\overrightarrow{P_1};0\right)$ and $(\sigma_2;1)$ laying on the conic C.

Let Ω_1 be the midpoint of the segment $[\sigma_0;\sigma_2]$.

Let h_1 defined by

$$h_1 : u \longmapsto \frac{\dfrac{\sqrt{2}}{2}(1-u)+u}{\sqrt{2}\,(1-u)+u} \tag{22}$$

then $\gamma \circ h_1$ is a Bézier curve with control mass points $(\sigma_{01};1)$, $(P_{11};\varpi_{11})$ and $(\sigma_{21};1)$ laying on

the conic C with:

$$\left\{\begin{array}{rcl}(\sigma_{01};1) & = & \left(\mathcal{T}_{\overrightarrow{P_1}}(\Omega_1);1\right)\\ (P_{11};\varpi_{11}) & = & \left(\mathcal{T}_{\overrightarrow{P_1}}(\sigma_2);\dfrac{\sqrt{2}}{2}\right)\\ (\sigma_{21};1) & = & (\sigma_2;1)\end{array}\right. \quad (23)$$

The Fig. 4 shows an iteration of the subdivision of a semi-circle based on the Theorems 3 and 4.

4.3.3 Synthesis

The Fig. 5 shows a graph which synthesizes the links between the theorems which permit the subdivisions of a connected circle (an ellipse with an Euclidean point of view).

5 Subdivision of a Dupin cyclide patch

In this section, the algorithms given in [15] are simplified using the representation of the brother circles on Λ^4. These curves are modeled using Bézier curves. The same method is applied to all ring Dupin cyclides (non-degenerate or torus). Let σ_0 and τ_0 be two representations of spheres which define the Dupin cyclide, if they do not belong to the same brother circle on Λ^4, then the light-like vector $\overrightarrow{\sigma_0\tau_0}$ defines the Dupin cyclide point.

Fig. 6 shows a subdivision of a Dupin cyclide patch. The first (resp. second) family of spheres is defined by the Bézier curve with control mass points $(\sigma_0;1)$, $(P_1;\omega_1)$ and $(\sigma_2;1)$ (resp. $(\tau_0;1)$, $(Q_1;\varpi_1)$ and $(\tau_2;1)$). The vertex P_{00}, P_{02}, P_{20} and P_{22} of the Dupin cyclide patch are defined by the light-like vectors $\overrightarrow{\sigma_0\tau_0}$, $\overrightarrow{\sigma_0\tau_2}$, $\overrightarrow{\sigma_2\tau_0}$ and $\overrightarrow{\sigma_2\tau_2}$.

First, the Bézier curve with control mass points $(\sigma_0;1)$, $(P_1;\omega_1)$ and $(\sigma_2;1)$ is subdivided to obtain the two Bézier curves with control mass points $(\sigma_0;1)$, $(P_{10};\omega_{10})$ and $(\sigma_{01};1)$ on one hand and $(\sigma_{01};1)$, $(P_{11};\omega_{11})$ and $(\sigma_2;1)$ on the other hand. Two new points P_{010} and P_{012} are computed in $\mathcal{E}_3$ by using the light-like vectors $\overrightarrow{\sigma_{01}\tau_0}$ and $\overrightarrow{\sigma_{01}\tau_2}$.

In the same way, the Bézier curve with control mass points $(\tau_0;1)$, $(Q_1;\varpi_1)$ and $(\tau_2;1)$ is subdivided to obtain the two Bézier curve with control mass points $(\tau_0;1)$, $(Q_{10};\varpi_{10})$ and $(\tau_{01};1)$ on one hand and $(\tau_{01};1)$, $(Q_{11};\varpi_{11})$ and $(\tau_2;1)$ on the other hand. Two new points P_{001} and P_{201} are computed in $\mathcal{E}_3$ by using the light-like vectors $\overrightarrow{\sigma_0\tau_{01}}$ and $\overrightarrow{\sigma_2\tau_{01}}$.

Finally, the point P_{0101} is computed in $\mathcal{E}_3$ by using the light-like vector $\overrightarrow{\sigma_{01}\tau_{01}}$. In Fig. 7, the patch of vertices $P_{00}P_{20}P_{22}P_{02}$ is replaced by the four patches of vertices

- P_{00}, P_{010}, P_{0101} and P_{001},
- P_{010}, P_{20}, P_{201} and P_{0101},
- P_{0101}, P_{201}, P_{22} and P_{012},
- P_{012}, P_{02}, P_{001} and P_{0101}.

The original spheres S_0 and S_2 are defined by the points σ_0 and σ_2 whereas the sphere S_{01} is defined by the construction of the point σ_{01}.

Using the same algorithm, the Fig. 8 shows the subdivision of a path of ring torus. Let us recall than in [15], the algorithms depend on the type of the surface (torus or non-degenerate Dupin cyclide) and then, the first work provides the determination of the Dupin cyclide. Moreover, there is two algorithms to subdivide a torus, one for the meridians and one for the parallels.

6 Conclusion and future works

In this paper, we have given methods to subdivide Bézier curves representing ellipse arc or semi-ellipse using mass points. These conics representing Dupin cyclides are circles on the space of spheres in the Minkowski-Lorentz space: one conic is a family of spheres which generates the Dupin cyclide i.e. a canal surface. Using the two circles, the same algorithms permit to subdivide Dupin cyclide patches too than can be used in patch surfaces.

In a second paper, we will give methods to subdivide Dupin cyclides having one or two singular points i.e. subdivide Bézier curves which represent parabolae or hyperbolae arcs in the usual Euclidean affine plane.

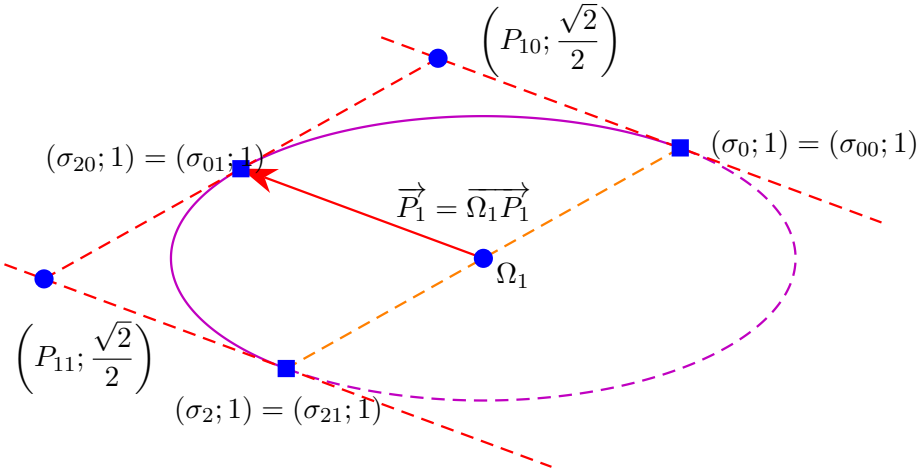

Figure 4: One iteration of a connected semi-circle defined by a BR curve of control mass points $(\sigma_0; 1)$, $\left(\overrightarrow{P_1}; 0\right)$ and $(\sigma_2; 1)$.

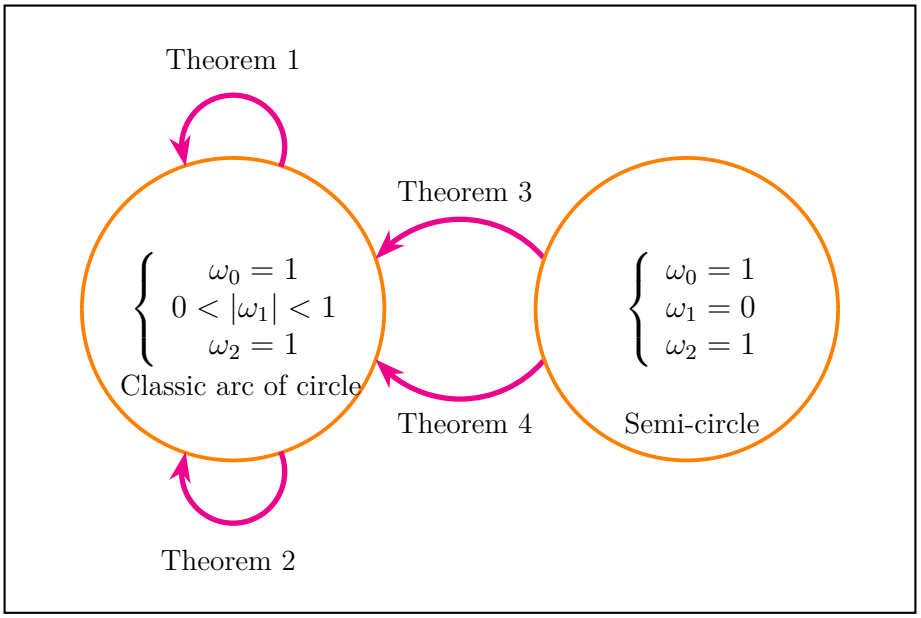

Figure 5: Graph which synthesizes the subdivisions of a connected circle (an ellipse with an Euclidean point of view).

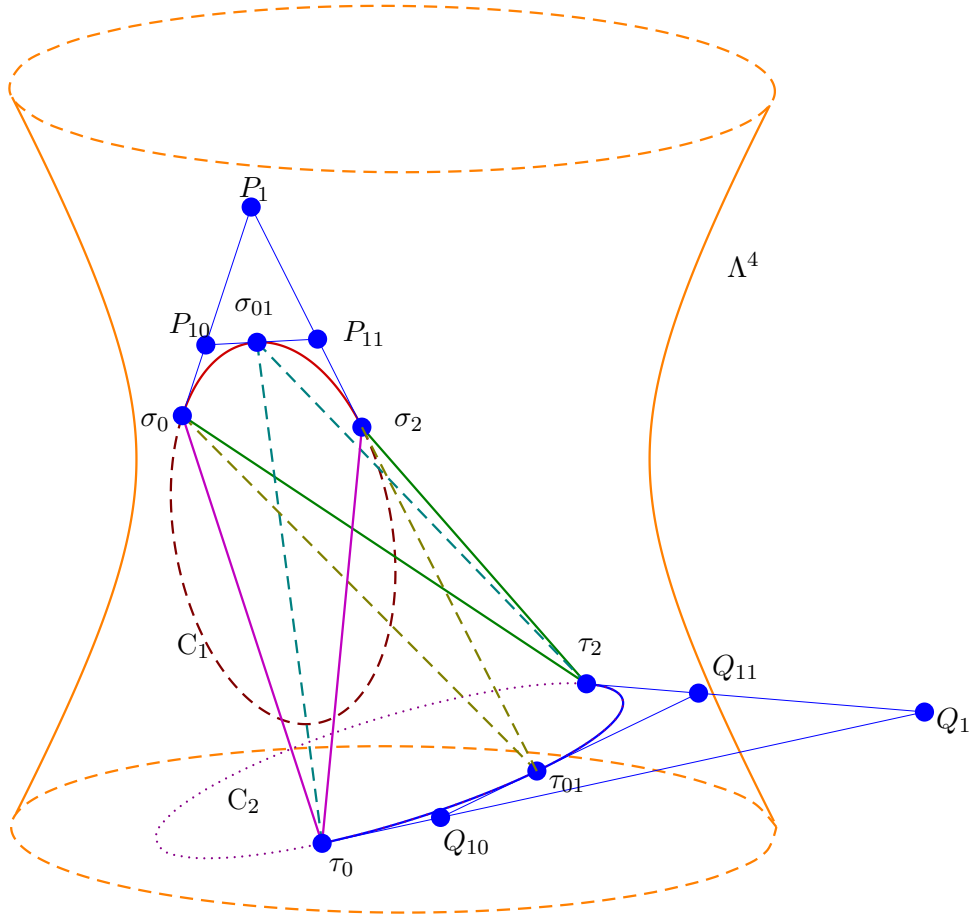

Figure 6: One iteration of a subdivision of a Dupin cyclide patch. Each Bézier curves represents the spheres whose Dupin cyclide is the envelope.

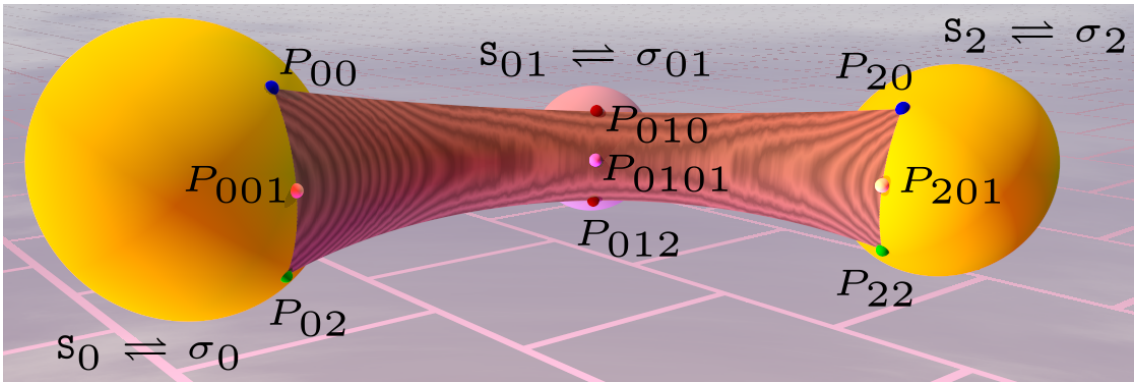

Figure 7: Subdivision of a Dupin cyclide patch: the patch of vertices $P_{00}P_{20}P_{22}P_{02}$ is replaced by the four patches of vertices $P_{00}P_{010}P_{0101}P_{001}$, $P_{010}P_{20}P_{201}P_{0101}$, $P_{0101}P_{201}P_{22}P_{012}$ and $P_{012}P_{02}P_{001}P_{0101}$.

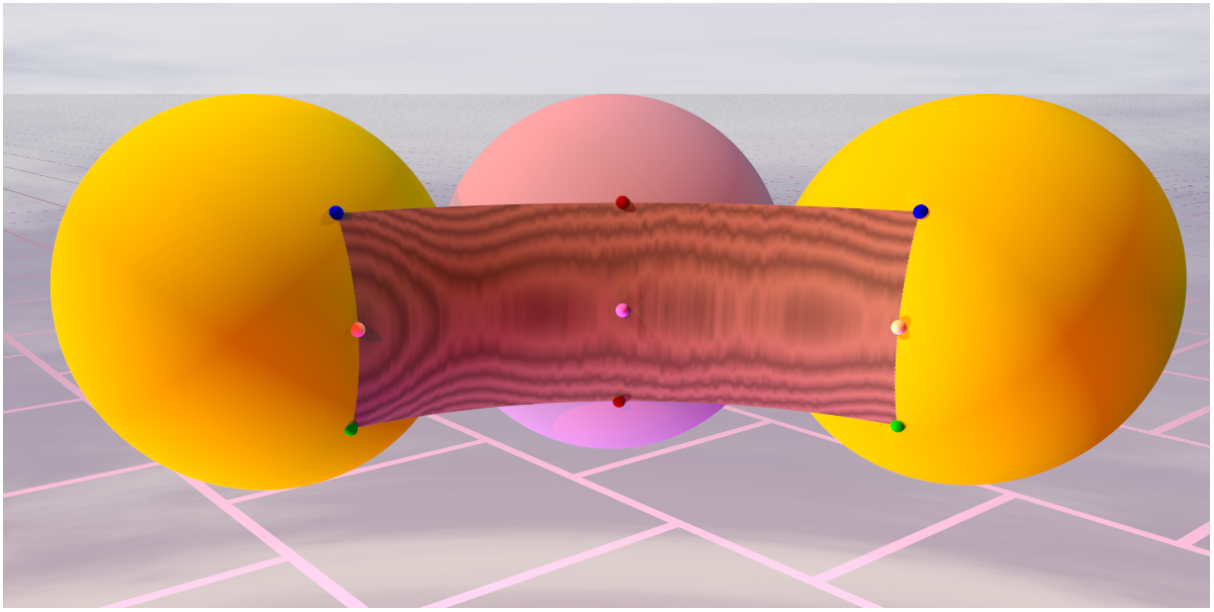

Figure 8: Subdivision of a path of ring torus.

References:

[1] C. P. Dupin. Application de Géométrie et de Méchanique à la Marine, aux Ponts et Chaussées, etc. Bachelier, Paris, 1822.

[2] R. R. Martin. Principal patches for computational geometry. PhD thesis, Engineering Department, Cambridge University, 1982.

[3] A. R. Forsyth. Lecture on Differential Geometry of Curves and Surfaces. Cambridge University Press, 1912.

[4] Gaston Darboux. Principes de géométrie analytique. Gauthier-Villars, 1917.

[5] G. Darboux. Sur une Classe Remarquable de Courbes et de Surfaces Algébriques et sur la Théorie des Imaginaires. Gauthier-Villars, 1873.

[6] M. Berger, M. Cole, and S. Levy. Geometry II. Number vol. 2 in Universitext (1979). Springer, 2009.

[7] M. J. Pratt. Cyclides in computer aided geometric design. Computer Aided Geometric Design, 7(1-4):221–242, 1990.

[8] K. Ueda. Normalized Cyclide Bézier Patches. In Mathematical Methods for Curves and Surfaces, pages 507–516, Nashville, USA, 1995. Vanderbilt University Press.

[9] G. Albrecht and W. Degen. Construction of Bézier rectangles and triangles on the symmetric Dupin horn cyclide by means of inversion. Computer Aided Geometric Design, 14(4):349–375, 1996.

[10] L. Garnier, S. Foufou, and M. Neveu. Conversion de cyclides de Dupin en carreaux de Bézier rationnels biquadriques. In Actes des 15^{emes} journées AFIG, pages 231–240, Lyon, France, December 2002.

[11] R. Martin. Principal Patches. A new class of surface patch based on differential geometry. In Eurographic's 1983, pages 47–55, 1983.

[12] Y. L. Srinivas, K. P. Vinod Kumar, and Debasish Dutta. Surface design using cyclide patches. Computer-aided Design, 28(4):263–276, 1996.

[13] Belbis Bertrand, Garnier Lionel, and Foufou Sebti. Construction of 3D triangles on Dupin cyclides. International Journal of Computer Vision and Image Processing (IJCVIP), 1(2):42–57, 2011.

[14] L. Garnier. Mathématiques pour la modélisation géométrique, la représentation 3D et la synthèse d'images. Ellipses, 2007. ISBN : 978-2-7298-3412-8.

[15] Lionel Garnier and Christian Gentil. Construction itérative de carreaux de cyclide de dupin et représentation par des g.i.f.s. affines. R.E.F.I.G., 5(2), Décembre 2011.

[16] L. Garnier, S. Foufou, and M. Neveu. Conversion d'un carreau de Bézier rationnel biquadratique en un carreau de cyclide de Dupin quartique. RTSI-TSI, 25(6):709–734, 2006. numéro spécial AFIG'04.

[17] L. Garnier and L. Druoton. Constructions of principal patches of Dupin cyclides defined by constraints : four vertices on a given circle and two perpendicular tangents at a vertex. In XIV Mathematics of Surfaces, pages 237–276, Birmingham, Royaume-Uni, 11-13 september 2013.

[18] P. Bézier. Courbe et surface, volume 4. Hermès, Paris, 2ème edition, Octobre 1986.

[19] P. De Casteljau. Mathématiques et CAO. Volume 2 : formes à pôles. Hermes, 1985.

[20] J. P. Bécar. Forme (BR) des coniques et de leurs faisceaux. PhD thesis, Université de Valenciennes et de Hainaut-Cambrésis, LIMAV, Décembre 1997.

[21] J. C. Fiorot and P. Jeannin. Courbes et surfaces rationnelles. Masson, 1989.

[22] J. P. Bécar and L. Garnier. Points massiques, courbes de Bézier quadratiques et coniques : un état de l'art. In G.T.M.G. 2014, Lyon, 26 au 27 mars 2014.

[23] Lionel Garnier and Jean-Paul Bécar. Mass points, Bézier curves and conics: a survey. In Eleventh International Workshop on Automated Deduction in Geometry, Proceedings of ADG 2016, pages 97–116, Strasbourg, France, June 2016. http://ufrsciencestech.u-bourgogne.fr/∼garnier/publications/adg2016/.

[24] M. Paluszny and W. Boehm. General cyclides. Computer Aided Geometric Design, 15(7):699–710, 1998.

[25] U. Hertrich-Jeromin. Introduction to M bius differential geometry. London Mat. Soc. Lecture note, Cambridge University Press, xii:300, 2003.

[26] T.E. Cecil. Lie sphere geometry. Universitext, 1992.

[27] R. Langevin and P.G. Walczak. Conformal geometry of foliations. Geom Dedicata, 132(5):135–178, 2008.

[28] Rémi Langevin, Jean-Claude Sifre, Lucie Druoton, Lionel Garnier, and Marco Paluszny. Finding a cyclide given three contact conditions. Computational and Applied Mathematics, 34:1–18, 2015.

[29] Lionel Garnier, Jean-Paul Bécar, Lucie Druoton, Laurent Fuchs, and Géraldine Morin. Theory of Minkowski-Lorentz Spaces, pages 1–17. Springer International Publishing, Cham, 2018.

[30] Lionel Garnier, Jean-Paul Bécar, and Lucie Druoton. Canal surfaces as Bézier curves using mass points. Computer Aided Geometric Design, 54:15–34, 2017.

[31] L. Druoton, L. Fuchs, L. Garnier, and R. Langevin. The non-degenerate Dupin cyclides in the space of spheres using geometric algebra. Advances in Applied Clifford Algebras, 23(4):787–990, 2014. ISSN 0188-7009.

[32] Leo Dorst, Daniel Fontijne, and Stephen Mann. Geometric Algebra for Computer Science: An Object-Oriented Approach to Geometry. Morgan Kaufmann Publishers Inc., San Francisco, CA, USA, 1st edition, 2007.

[33] L. Druoton, L. Garnier, and R. Langevin. Iterative construction of Dupin cyclide characteristic circles using non-stationary Iterated Function Systems (IFS). Computer-Aided Design, 45(2):568–573, February 2013. Solid and Physical Modeling 2012, Dijon.

[34] L. Druoton, R. Langevin, and L. Garnier. Blending canal surfaces along given circles using Dupin cyclides. International Journal of Computer Mathematics, pages 1–20, 2013.

[35] J. C. Fiorot and P. Jeannin. Rational Curves and Surfaces: Applications to CAD. John Wiley and Sons Ltd, 1992.

[36] Ron Goldman. On the algebraic and geometric foundations of computer graphics. ACM Trans. Graph., 21(1):52–86, January 2002.

[37] D. Dutta, R. R. Martin, and M. J. Pratt. Cyclides in surface and solid modeling. IEEE Computer Graphics and Applications, 13(1):53–59, January 1993.

[38] L. Druoton, L. Garnier, R. Langevin, F. Sulpice, and R. Besnard. Les cyclides de Dupin et l'espace des sphères. AFIG 2010, pages 147–155, 2010.

[39] L. Druoton, L. Garnier, R. Langevin, and F. Sulpice. Les cyclides de Dupin et l'espace des sphères. REFIG, 5(1):41–59, 2011.

[40] L. Garnier. Constructions euclidiennes, dans le plan affine, d'arcs de coniques propres par des I.F.S. affines non stationnaires. Revue Electronique Francophone d'Informatique Graphique, 4(1):21–56, 2010.

[41] Jean-Paul Bécar, Laurent Fuchs, and Lionel Garnier. Courbe d'une fraction rationnelle et courbes de b zier points massiques. Toulouse, France, 20-21 mars 2019. Université de Toulouse.

Appendices

A Recalls of Minkowski-Lorentz space and space of spheres

The Minkowski-Lorentz space is a generalization of the Spacetime used in Einstein's relativity theory.

A.1 Construction of Minkowski-Lorentz space and space of spheres

The Minkowski-Lorentz space $\overrightarrow{\mathrm{L}_{4,1}}$ is the real vector space of dimension 5. The symmetric bilinear form $\mathcal{L}_{4,1}$ denoted by a dot product, is defined on the canonical basis $(\overrightarrow{e_-}, \overrightarrow{e_1}, \overrightarrow{e_2}, \overrightarrow{e_3}, \overrightarrow{e_+})$ as follows

$$\begin{cases} \overrightarrow{e_i} \cdot \overrightarrow{e_j} &= 0 \text{ if } i \neq j \\ \overrightarrow{e_-} \cdot \overrightarrow{e_-} &= -1 \\ \overrightarrow{e_i} \cdot \overrightarrow{e_i} &= 1 \text{ if } i \neq - \end{cases} \tag{24}$$

with $i \in \{1, 2, 3, +\}$ and $j \in \{-, 1, 2, 3, +\}$.

The affine Minkowski-Lorentz space $\mathrm{L}_{4,1}$ is defined by the point $O_5 = (0, 0, 0, 0, 0)$ and $\overrightarrow{\mathrm{L}_{4,1}}$.

A new basis $(\overrightarrow{e_o}, \overrightarrow{e_1}, \overrightarrow{e_2}, \overrightarrow{e_3}, \overrightarrow{e_\infty})$ with

$$\begin{cases} \overrightarrow{e_o} = \overrightarrow{e_-} - \overrightarrow{e_+} \\ \overrightarrow{e_\infty} = \frac{1}{2}\left(\overrightarrow{e_-} + \overrightarrow{e_+}\right) \end{cases}$$

eases to embed the usual 3D Euclidean affine space $\mathcal{E}_3$ in the Minkowski-Lorentz space. The

reader will check that

$$\overrightarrow{e_o} \centerdot \overrightarrow{e_o} = \overrightarrow{e_\infty} \centerdot \overrightarrow{e_\infty} = 0$$

and

$$\overrightarrow{e_o} \centerdot \overrightarrow{e_\infty} = -1$$

The origin point O_3 of $\mathcal{E}_3$ is obtained by $\overrightarrow{e_o} = \overrightarrow{O_5O_3}$ and the vector $\overrightarrow{e_\infty}$ represents the point at infinity of $\mathcal{E}_3$.

According to Minkowski definitions, any vector $\overrightarrow{u} \in \overrightarrow{\mathrm{L}_{4,1}}$ such that $\overrightarrow{u}^2$ is negative, positive or zero is qualified as a time-like, space-like or light-like vector respectively. The light-cone C_l is the set of the points M which verify

$$\overrightarrow{O_5M}^2 = 0 \tag{25}$$

i.e. $\overrightarrow{O_5M}$ is an isotropic vector, is perpendicular to itself, and the pseudo-distance between O_5 and M is null.

A.2 Equivalent representations of elements in $\mathcal{E}_3$ and Minkowski-Lorentz space

The Table 2 gives important Formulae to determine the representation of elements of $\mathcal{E}_3$. The space of spheres Λ^4 is the set of points σ such as $\overrightarrow{O_5\sigma}^2 = 1$. This space represents the oriented spheres and oriented planes of $\mathcal{E}_3$.

A.3 Properties of points and spheres

The Table 3 gives some properties of the representations of element of $\mathcal{E}_3$ in the Minkowski-Lorentz spaces. If the orientation of the tangent spheres S_1 and S_2 at P is the same, then

$$\overrightarrow{O_5\sigma_1} \centerdot \overrightarrow{O_5\sigma_2} = 1 \tag{26}$$

and

$$\overrightarrow{\sigma_1\sigma_2}^2 = 0 \tag{27}$$

and the vectors $\overrightarrow{\sigma_1\sigma_2}$ and $\overrightarrow{p}$ are parallel. Moreover, the direction of the vector $\overrightarrow{\sigma_1\sigma_2}$ in $\overrightarrow{\mathrm{L}_{4,1}}$ defines, in $\mathcal{E}_3$, the point of tangency between the spheres S_1 and S_2.

A one parameter family of oriented spheres is a curve on Λ^4. The derivative spheres can be defined as follows.

Definition 2 : Derivative sphere

Let γ be a $\mathcal{C}^1$ curve, defined on an interval I, on Λ^4. The parameterization of the curve satisfies the following conditions:

- the curve is at least $\mathcal{C}^1$;
- the tangent vectors to the curve are always space-like vectors.

The intersection between Λ^4 and the line defined by O_5 and $\overrightarrow{\frac{\partial\gamma}{\partial\theta}}(\theta_0)$ is a sphere $\overset{\bullet}{\gamma}(\theta_0)$ which is orthogonal to the sphere $\gamma(\theta_0)$ e.g.

$$\overrightarrow{O_5\ \overset{\bullet}{\gamma}(\theta_0)} \centerdot \overrightarrow{O_5\gamma(\theta_0)} = 0 \tag{28}$$

Moreover, if $\overset{\bullet}{\gamma}(\theta_0)$ (resp. $\gamma(\theta_0)$) represents the sphere $\overset{\bullet}{\mathrm{S}}$ (resp. S), then $\overset{\bullet}{\mathrm{S}} \cap \mathrm{S}$ is a circle, called characteristic circle if γ models a canal surface. The canal Surface and the sphere $\gamma(\theta_0)$ are tangent along the circle $\overset{\bullet}{\mathrm{S}} \cap \mathrm{S}$.

B Mass points and Minkowski-Lorentz spaces

B.1 The set of mass points

A mass point is a couple (M, m) such that: if the mass m is equal to 0, $\overrightarrow{M}$ is a vector belonging to $\overrightarrow{\mathrm{L}_{4,1}}$ otherwise M is a point belonging to the affine space $\mathrm{L}_{4,1}$. So, a mass point is a weighted point or a vector and the set of these mass points is denoted $\widetilde{\mathrm{L}_{4,1}}$ i.e.

$$\widetilde{\mathrm{L}_{4,1}} = \overrightarrow{\mathrm{L}_{4,1}} \times \{0\} \cup \mathrm{L}_{4,1} \times \mathbb{R}^* \tag{29}$$

The notation $Bar\{(M;\omega);(N;\mu)\}$ denotes the barycenter of the weighted points $(M;\omega)$ and $(N;\mu)$ and for any points A and B in $\mathrm{L}_{4,1}$ we have:

$$Bar\{(A;-1);(B;1)\} \quad \text{is} \quad \overrightarrow{AB} \in \overrightarrow{\mathrm{L}_{4,1}} \tag{30}$$

We define a stable addition $\oplus$ in $\widetilde{\mathrm{L}_{4,1}}$, such that $\left(\widetilde{\mathrm{L}_{4,1}}, \oplus\right)$ is a commutative group:

Table 2: correspondence between elements of $\mathcal{E}_3$ and points or vectors in the Minkowski-Lorentz spaces

Type	$\mathcal{E}_3 \cup \{\infty\}$	$\mathrm{L}_{4,1}$ or $\overrightarrow{\mathrm{L}_{4,1}}$	Property
Point	$P \in \mathcal{E}_3$	$\overrightarrow{p} = \overrightarrow{e_o} + \overrightarrow{O_3P} + \frac{\left\|\overrightarrow{O_3P}\right\|^2}{2}\overrightarrow{e_\infty}$	$\overrightarrow{p}^2 = 0$
	∞	$\overrightarrow{e_\infty}$	$\overrightarrow{e_\infty}^2 = 0$
Sphere	Center Ω	$\overrightarrow{O_5\sigma} = \frac{1}{\rho}\left(\overrightarrow{e_o} + \overrightarrow{\Omega} + \frac{1}{2}\left(\left\|\overrightarrow{\Omega}\right\|^2 - \rho^2\right)\overrightarrow{e_\infty}\right)$	$\overrightarrow{O_5\sigma}^2 = 1$
	Radius ρ		
Plane $\mathrm{L}_{4,1}$	Normal vector $\overrightarrow{N}$	$\overrightarrow{O_5\pi} = \overrightarrow{N} + \left(\overrightarrow{N} \bullet \overrightarrow{P}\right)\overrightarrow{e_\infty}$	$\overrightarrow{O_5\pi}^2 = 1$
	Point $P \in \mathrm{L}_{4,1}$		

Table 3: Properties of the representations of points, planes and spheres in Minkowski-Lorentz spaces.

Type	$\mathcal{E}_3 \cup \{\infty\}$	$\mathrm{L}_{4,1}$ or $\overrightarrow{\mathrm{L}_{4,1}}$	Property
Point	P	$\overrightarrow{p}$	$P \in \mathrm{S} \Longleftrightarrow \overrightarrow{p} \,.\, \overrightarrow{O_5\sigma} = 0$
Sphere	S	$\sigma \in \Lambda^4$	$P \in \mathrm{L}_{4,1} \Longleftrightarrow \overrightarrow{p} \,.\, \overrightarrow{O_5\pi} = 0$
Plane	$\mathcal{P}$	$\pi \in \Lambda^4$	$\overrightarrow{e_\infty} \,.\, \overrightarrow{O_5\pi} = 0$
Sphere	S_1	σ_1	$\mathrm{S}_1 \perp \mathrm{S}_2 \Longleftrightarrow \overrightarrow{O_5\sigma_1} \,.\, \overrightarrow{O_5\sigma_2} = 0$
			$\#\left(\mathrm{S}_1 \cap \mathrm{S}_2\right) > \{1\} \Longleftrightarrow \left\|\overrightarrow{O_5\sigma_1} \,.\, \overrightarrow{O_5\sigma_2}\right\| < 1$
Sphere	S_2	σ_2	S_1 and S_2 are tangent$\Longleftrightarrow \left\|\overrightarrow{O_5\sigma_1} \,.\, \overrightarrow{O_5\sigma_2}\right\| = 1$
			$\mathrm{S}_1 \cap \mathrm{S}_2 = \emptyset \Longleftrightarrow \left\|\overrightarrow{O_5\sigma_1} \,.\, \overrightarrow{O_5\sigma_2}\right\| > 1$

- $(M;\omega) \oplus (N;-\omega) = \left(\omega\ \overrightarrow{NM}; 0\right)$;
- $(\overrightarrow{u};0) \oplus (\overrightarrow{v};0) = (\overrightarrow{u}+\overrightarrow{v};0)$;
- if $\omega \neq 0$ and $\omega + \mu \neq 0$, then $(M;\omega) \oplus (N;\mu) = \left(Bar\left\{(M;\omega);(N;\mu)\right\};\omega+\mu\right)$;
- if $\omega \neq 0$ then $(M;\omega) \oplus (\overrightarrow{u};0) = \left(\mathcal{T}_{\frac{1}{\omega}\overrightarrow{u}}(M);\omega\right)$ where $\mathcal{T}_{\overrightarrow{w}}$ is the translation of $\mathrm{L}_{4,1}$ of vector $\overrightarrow{w}$.

In order to define $\left(\widetilde{\mathrm{L}_{4,1}}, \oplus, \odot\right)$ as a vector space, we define the multiplication by a scalar $\odot$ as follow:

- if $\omega \neq 0$, $0 \odot (M;\omega) = \left(\overrightarrow{0};0\right)$
- $\alpha \neq 0 \Longrightarrow \alpha \odot (M;\omega) = (M;\alpha\,\omega)$
- $\alpha \odot (\overrightarrow{u};0) = (\alpha\,\overrightarrow{u};0)$

For more details on the space of mass points, the reader can refer to books of Fiorot and Jeannin [21, 35] or the paper of Garnier and al. [30, 23].

B.2 Rational quadratic Bézier curves in $\widetilde{\mathrm{L}_{4,1}}$

B.2.1 Definition

Let us recall the definition of quadratic Bernstein polynomials

$$\left\{ \begin{array}{c} B_0(t) = (1-t)^2, \\ B_1(t) = 2\,t\,(1-t), \\ B_2(t) = t^2 \end{array} \right. \tag{31}$$

with $t \in [0,1]$.

Now, we can define a rational quadratic Bézier curves with three control mass points $(P_0;\omega_0)$, $(P_1;\omega_1)$ and $(P_2;\omega_2)$:

Definition 3 : Rational quadratic Bézier curve (BR curve) in $\widetilde{\mathrm{L}_{4,1}}$.
Let ω_0, ω_1 and ω_2 be three non-zero values.

Let $(P_0;\omega_0)$, $(P_1;\omega_1)$ and $(P_2;\omega_2)$ be three mass points in $\widetilde{\mathrm{L}_{4,1}}$, these points are not collinear.

Let us define two sets

$$\left\{ \begin{array}{rcl} I & = & \{i \in [\![0,2]\!] \mid \omega_i \neq 0\} \\ J & = & \{i \in [\![0,2]\!] \mid \omega_i = 0\} \end{array} \right. \tag{32}$$

Let us define the function ω_f as follows

$$\begin{array}{rccc} \omega_f : & [0,1] & \longrightarrow & \mathbb{R} \\ & t & \longmapsto & \displaystyle\sum_{i\in I} \omega_i \times B_i(t) \end{array} \tag{33}$$

A mass point $(M;\omega)$ or $(\overrightarrow{u};0)$ belongs to the quadratic Bézier curve defined by the three control mass points $(P_0;\omega_0)$, $(P_1;\omega_1)$ and $(P_2;\omega_2)$, if there is a parameter t_0 in $[0;1]$ such that:

- if $\omega_f(t_0) \neq 0$ then we have

$$\left\{ \begin{array}{rcl} \overrightarrow{OM} & = & \dfrac{1}{\omega_f(t_0)} \left(\displaystyle\sum_{i\in I} \omega_i\, B_i(t_0)\, \overrightarrow{OP_i} \right) \\ & + & \dfrac{1}{\omega_f(t_0)} \left(\displaystyle\sum_{i\in J} B_i(t_0)\, \overrightarrow{P_i} \right) \\ \omega & = & \omega_f(t_0) \end{array} \right. \tag{34}$$

- if $\omega_f(t_0) = 0$ then we have

$$\begin{array}{rcl} \overrightarrow{u} & = & \sum_{i\in I} \omega_i B_i(t_0)\, \overrightarrow{OP_i} \\ & + & \sum_{i\in J} B_i(t_0)\, \overrightarrow{P_i} \end{array} \tag{35}$$

Note that a Bézier curve with mass points of control mixes affine properties

$$\frac{1}{\displaystyle\sum_{i\in I} \omega_i\, B_i(t_0)} \left(\sum_{i\in I} B_i(t_0)\ \omega_i\, \overrightarrow{OP_i} \right) \tag{36}$$

and vector properties

$$\frac{1}{\omega_f(t_0)} \left(\sum_{i\in J} B_i(t_0)\ \overrightarrow{P_i} \right) \tag{37}$$

B.2.2 Some properties

If $J = \emptyset$, we do not modify the Bézier curve if we multiply all the weights by a non-zero constant value. More generally, the following lemma holds:

Lemma 1 Let $(P_0;\omega_0)$, $(P_1;\omega_1)$ and $(P_2;\omega_2)$ be three mass points $\widetilde{\mathrm{L}_{4,1}}$.

Let λ be a non-zero value.

If $\displaystyle\sum_{i\in I} \omega_i\, B_i(t_0) \neq 0$, we have

$$\begin{array}{c} BR\left\{ (P_i;\omega_i)_{i\in I}\,;\, \left(\overrightarrow{P_j};0\right)_{j\in J} \right\} = \\ BR\left\{ (P_i;\lambda\,\omega_i)_{i\in I}\,;\, \left(\lambda\,\overrightarrow{P_j};0\right)_{j\in J} \right\} \end{array} \tag{38}$$

Proof:

$$\begin{aligned}
&\frac{1}{\sum_{i\in I}\omega_i \times B_i(t_0)}\left(\sum_{i\in I}\omega_i B_i(t_0)\overrightarrow{OP_i}\right) \quad + \\
&\frac{1}{\sum_{i\in I}\omega_i \times B_i(t_0)}\left(\sum_{j\in J}B_j(t_0)\overrightarrow{P_i}\right) \quad = \\
&\frac{1}{\sum_{i\in I}\lambda\omega_i \times B_i(t_0)}\left(\sum_{i\in I}\lambda\omega_i B_i(t_0)\overrightarrow{OP_i}\right) \quad + \\
&\frac{1}{\sum_{i\in I}\lambda\omega_i \times B_i(t_0)}\left(\sum_{j\in J}\lambda B_j(t_0)\overrightarrow{P_i}\right)
\end{aligned}$$

■

Without loss of generality, using Theorem 5, if a weight is equal to 0, the others weights belong to $\{0,1\}$. The table 4 gives the type of the conic defined by a quadratic Bézier curve with mass points.

B.2.3 Homographic Parameter Change

The Bézier curve and the Bézier curve obtained by this homographic parameter change model two different arcs of the same given conic.

Theorem 5 : Homographic Parameter Change

Let γ be a Bézier curve with control mass points $(P_0;\omega_0)$, $(P_1;\omega_1)$ and $(P_2;\omega_2)$ laying on the conic C. Let a, b, c and d be four real numbers satisfying

$$\left|\begin{array}{cc} a & b \\ c & d \end{array}\right| \neq 0 \tag{39}$$

Let h be defined by

$$\begin{array}{rccc} h: & \overline{\mathbb{R}} & \longrightarrow & \overline{\mathbb{R}} \\ & u & \longmapsto & \dfrac{a\,(1-u)+b\,u}{c\,(1-u)+d\,u} \end{array} \tag{40}$$

then $\gamma \circ h$ is a Bézier curve of control mass points $(Q_0;\varpi_0)$, $(Q_1;\varpi_1)$ and $(Q_2;\varpi_2)$ with

$$\left\{\begin{array}{rcl}
(Q_0;\varpi_0) & = & \\
(c-a)^2 \odot (P_0;\omega_0) & \oplus & \\
2\,a\,(c-a) \odot (P_1;\omega_1) & \oplus & \\
a^2 \odot (P_2;\omega_2) & & \\
(Q_1;\varpi_1) & = & \\
(c-a)\,(d-b) \odot (P_0;\omega_0) & \oplus & \\
(b\,c-2\,a\,b+a\,d) \odot (P_1;\omega_1) & \oplus & \\
a\,b \odot (P_2;\omega_2) & & \\
(Q_2;\varpi_2) & = & \\
(d-b)^2 \odot (P_0;\omega_0) & \oplus & \\
2\,b\,(d-b) \odot (P_1;\omega_1) & \oplus & \\
b^2 \odot (P_2;\omega_2) & &
\end{array}\right. \tag{41}$$

Proof: see [20, 41]. ■

The following corollary of Theorem 5 offers to keep the endpoints.

Corollary 1 : Homographic Parameter Change with 0 and 1 unmodified.

Let γ be a Bézier curve with mass control points $(P_0;\omega_0)$, $(P_1;\omega_1)$ and $(P_2;\omega_2)$ laying on the conic C. Let b and c be two non-zero numbers. Let h be defined by :

$$\begin{array}{rccc} h: & \overline{\mathbb{R}} & \longrightarrow & \overline{\mathbb{R}} \\ & u & \longmapsto & \dfrac{b\,u}{c\,(1-u)+b\,u} \end{array} \tag{42}$$

then $\gamma \circ h$ is a Bézier curve with mass control points $(Q_0;\varpi_0)$, $(Q_1;\varpi_1)$ and $(Q_2;\varpi_2)$ on the same conic C with

$$\left\{\begin{array}{rcl}
(Q_0;\varpi_0) & = & c^2 \odot (P_0;\omega_0) \\
(Q_1;\varpi_1) & = & b\,c \odot (P_1;\omega_1) \\
(Q_2;\varpi_2) & = & b^2 \odot (P_2;\omega_2)
\end{array}\right. \tag{43}$$

Proof: see [20].

Table 4: Type of the conic according the weights of the control mass points.

Weights $(\omega_0, \omega_1, \omega_2)$	$\Delta = \omega_1^2 - \omega_2\,\omega_0$	Euclidean type of the conic
$(1;\omega_1;1)$	$+$	$\omega_1 > 1$: connected hyperbola arc
	0	$\omega_1 = 1$: connected parabola arc
	$-$	$\omega_1 = 0$: semi-ellipse
	$-$	$0 < \lvert\omega_1\rvert < 1$: ellipse arc
	0	$\omega_1 = -1$: not connected parabola arc
	$+$	$\omega_1 < -1$: not connected hyperbola arc
$(0;1;1)$ or $(1;1;0)$	1	connected hyperbola arc
$(0;0;1)$ or $(1;0;0)$	0	connected parabola arc
$(0;1;0)$	1	hyperbola branch

The denominator of a rational quadratic Bézier curve defined by the mass points $(P_0;\omega_0)$, $(P_1;\omega_1)$ and $(P_2;\omega_2)$ is

$$(\omega_0 - 2\,\omega_1 + \omega_2)\,t^2 + 2\,(\omega_1 - \omega_0)\,t + \omega_0 \quad (44)$$

and the sign of the discriminant of this polynomial is

$$\omega_1^2 - \omega_2\,\omega_0 \quad (45)$$